



ELSEVIER

Available online at www.sciencedirect.com

SCIENCE @ DIRECT®

Nuclear Instruments and Methods in Physics Research A 542 (2005) 22–27

NUCLEAR
INSTRUMENTS
& METHODS
IN PHYSICS
RESEARCH
Section A

www.elsevier.com/locate/nima

Neutron-, gamma- and X-ray three-dimensional computed tomography at the Budapest research reactor site

Márton Balaskó^{a,*}, Attila Kuba^b, Antal Nagy^b, Zoltán Kiss^b,
Lajos Rodek^b, László Ruskó^b

^aKFKI Atomic Energy Research Institute H-1525 Budapest P.O. Box 49, Hungary

^bDepartment of Image Processing and Computer Graphics, University of Szeged, Árpád tér 2, Szeged, H-6720, Hungary

Available online 2 February 2005

Abstract

A new complex, neutron-, gamma- and X-ray three-dimensional computer tomography system suitable for experimental and industrial applications has been built at the 10-MW Budapest research reactor site. After the system was installed, a number of objects were investigated and tomographic projections were made. The evaluation relied on two reconstruction approaches. One of these is the classical, filtered back-projection method using 180 projected pictures, while the other is based on discrete tomography optimization algorithms where fewer projections were needed. © 2005 Elsevier B.V. All rights reserved.

PACS: 7.59.Fm; 87.59.Hp; 87.59.Jq

Keywords: Neutron-, Gamma- and X-ray tomography; Visco clutch

1. Introduction

In some situations it is important to know the three-dimensional (3D) structure of some objects and their current state. Nowadays 3D computed tomography (3D CT) is an indispensable tool for this problem and in research work, not to mention in the development of high-tech industrial tech-

nology. It is one the most versatile non-destructive testing (NDT) methods available. In Hungary, a new neutron-, gamma- and X-ray 3D CT system for applied use has been built at the 10-MW Budapest research reactor site. The source of the neutron (thermal and epithermal) radiation and gamma radiation was the reactor core, while the source of the X-ray radiation was a portable industrial X-ray generator whose power output lay between 50 kV; 5 mA and 300 kV; 5 mA. For neutron radiography imaging, a ZnS:Ag:Li⁶F converter screen was used. For gamma radio-

*Corresponding author. Tel.: +36 1 392 2222;
fax: +36 1 395 9162.

E-mail address: balasko@sunserv.kfki.hu (M. Balaskó).

graphy imaging, a NaCs single crystal was employed, and for X-ray radiography imaging, a ZnS converter screen (LGG 400 type) was used. The radiography pictures were made by a Peltier-cooled CCD camera, which was controlled by a PC with Image ProLite software. The first set of objects to be inspected was a series of reference cylinders followed by a VISCO clutch and Vidicon tube. The evaluation activity was carried out using two reconstruction procedures. One of these is the classical filtered back-projection method which uses 180 uniformly projected pictures (taken 1° at a time). The other is based on discrete tomography [1] optimization algorithms, where only a few (e.g. four) projections were required.

The main steps of the classical procedure involved median filtering, background correction, uniformity correction, and the reconstruction of tomographic sections using SNARK93 [6] software. When we applied discrete tomography [1], we supposed that the following information about an object to be reconstructed was available:

- the absorption coefficients of the constituent components (e.g., aluminum and water) were given,
- the cross-sections here could be described by circles.

2. Experimental procedure

Measurements were performed at the radiography station of the 10-MW Budapest research reactor site [2–4]. Near the reactor core the neutron flux was $10^8 \text{ n cm}^{-2} \text{ sec}^{-1}$, and the gamma radiation intensity was 8.3 Gyh^{-1} . The beam of the radiography station pointed directly into the reactor core. For this reason both the neutron and gamma spectra were white spectra containing a wide range of different energies. The radiation channel contained a complex, sandwich style collimator of diameter 25 mm which was able to generate the neutron and gamma beams at the same time. The collimator ratio (L/D) was 190 and the beam diameter was 230 mm in the exposure

plane. As mentioned above, the X-rays were produced by a portable industrial X-ray device. The CCD chip for radiography imaging had 512×512 pixels and sampled at a rate of 40 frames/s. The camera type was a Mono Cool View made by Photonic Science Limited. The objects we tested were placed on a robust goniometer table of a neutron stress diffractometer and could be rotated by a PC-controlled stepper motor. The tomographic tests were performed using a 400×400 image matrix with a field of view of 175 mm. 180 projections were taken by rotating the table in 1° angular increments. The set-up of the radiography apparatus used is shown in Fig. 1.

3. Objects investigated

Three objects were studied. The first was a reference cylinder to test the precision of the reconstruction. Then experiments were performed on two complex objects whose details are described below.

3.1. Reference cylinder

A series of cylinders were specially designed to test the reconstruction procedure. They were made of aluminium, iron and Plexi-Glass. Each of them had three drilled holes of different diameters and

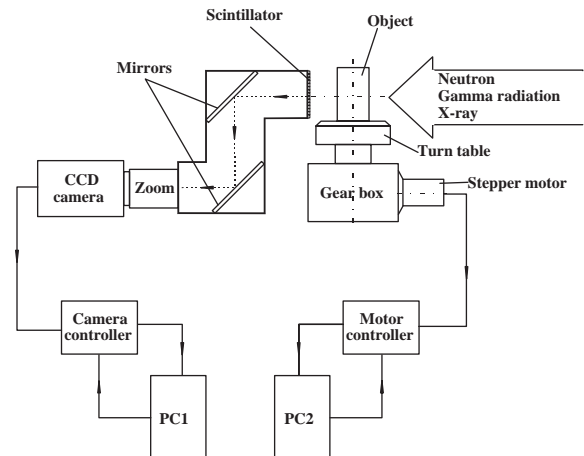


Fig. 1. Experimental arrangement of tomography system.

depths, whose holes had an asymmetric arrangement (see Fig. 2). This cylinder arrangement provided the ideal opportunity for us to apply our new discrete tomography technique. In the tests, an aluminium reference cylinder was used.

The hole with the biggest diameter was partially filled with acetone, while the two others contained water of different heights.

3.2. VISCO clutch

VISCO clutches are used to transfer torque from the vehicle engine to wheels, especially in four-wheel drive systems. The object we tested had a diameter of 150 mm, height of 100 mm and a 5 mm wall thickness. It was made of stainless steel and contained 24 pairs of 0.8-mm-thick metal plates.

The distance between two plates forming one pair was 0.4 mm and the distance between neighbouring pairs was 1 mm. The unit was partially filled with silicon oil to simulate lubricat-

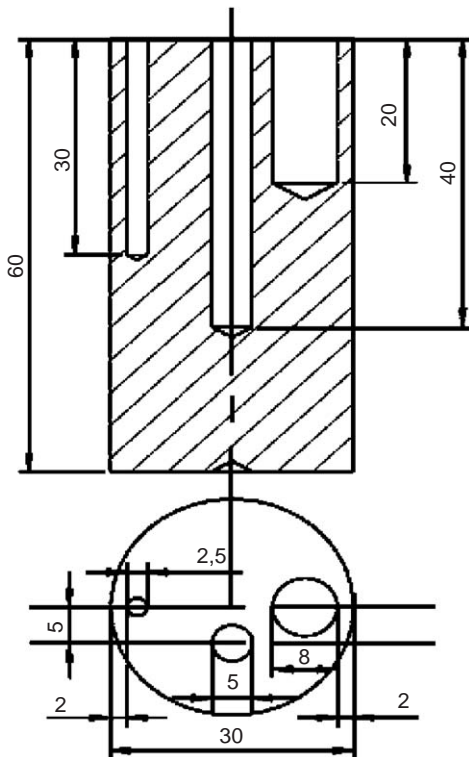


Fig. 2. Side view and plan view of the reference cylinder used.

ing oil. Fig. 3 shows the VISCO clutch used during the tomography test. Behind it can be seen the holder of the scintillator screen with the light shielding tube of the CCD camera.

3.3. Vidicon tube

The Vidicon tube is the most important part of a large, conventional TV camera. Its task is to turn visual data about the object into a corresponding electronic signal. Its wall which is made of glass covered by a getter material, is shown in Fig. 4.



Fig. 3. VISCO clutch on the rotating table used in the tomographic experiments.



Fig. 4. The Vidicon tube.

The tube here had a diameter of 28 mm, height of 178 mm, and a 0.3 mm wall thickness. It contained a large number of metal electrodes, an electron gun, accelerator rings and a photo cathode. In addition it had a built-in image intensifier on the front.

4. Experimental procedure

The reference cylinder was first used to test the precision of our reconstruction approach. Then neutron- and gamma-ray projections of the Visco clutch were made to provide information about the object. Following this, we made X-ray projections in order to learn about the arrangement of the electrodes in the Vidicon tube. The projection data obtained from using these three types of radiation together provide complementary information about the tube being examined.

Due to the distorting properties of the image acquiring system, some correction (so-called pre-processing) methods were applied to improve the projection images and to prepare them for reconstruction. The distortions encountered here are described in another paper [5]. In the first two cases the following correction steps were applied:

1. *Cropping*: We extract the relevant area of the projections containing the object under investigation.
2. *Intensity correction*: This is needed to achieve a roughly constant average background intensity.
3. *Uniformity correction*: This is done to eliminate the non-uniform sensitivity of the detector plate in the field of view.
4. *Thresholded median filtering*: This is done to eliminate high-intensity pixels.

4.1. Reference cylinder

The projection images using neutron particles were taken, one of which after preprocessing is shown in Fig. 5a. The size of each image was 365×400 pixels.

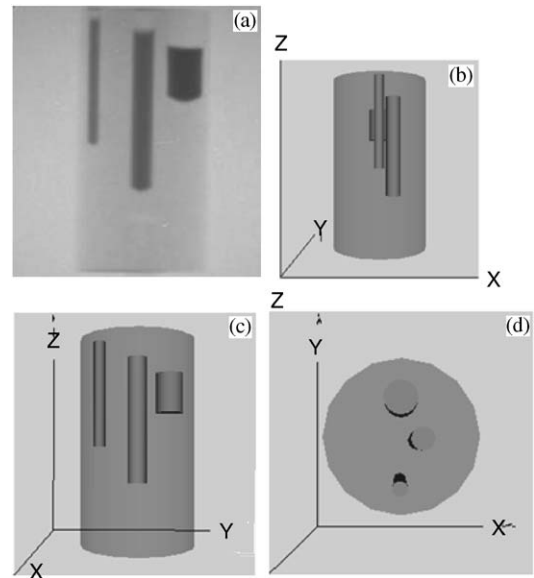


Fig. 5. 3D visualisation of the reconstructed cylinder. (a) One of the neutron radiography images, (b) 0° perspective view of the reconstructed cylinder, (c) 90° perspective view of the reconstructed cylinder and (d) plan view of the reconstructed cylinder.

The reconstruction was performed using the parametric reconstruction technique described in Ref. [5], which only needed four projections. As mentioned above, our method makes use of the following two facts: (i) the object to be reconstructed is composed of a known number of cylinders, and (ii) the absorption coefficients of the materials are approximately known. The resulting 3D model was stored in a VRML file. A visual representation of the result is given in Fig. 5.

4.2. VISCO clutch

One projection image of the sequence we obtained using neutron particles is shown in Fig. 6a following preprocessing. The exposure time for each was 3 s/projection image.

We should mention here that this clutch contained some residual silicon oil after being emptied. We should also remark that some

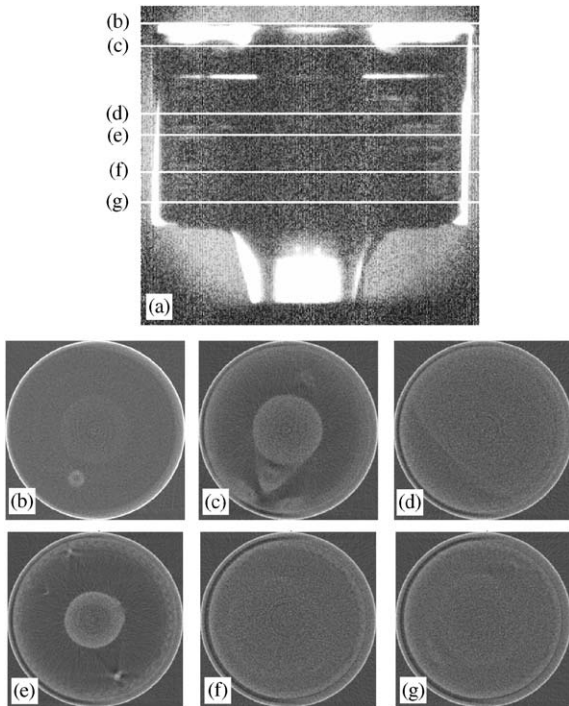


Fig. 6. Results of the reconstruction of the VISCO clutch using 180 neutron-ray images. (a) One of the projection images after intensity and uniformity corrections and (b–g) cross-sections reconstructed by filtered back-projection using a cosine filter.

brightness and contrast adjustments were applied to each image for suitable visualisation.

Next, the neutron- and gamma-ray projections were reconstructed using the SNARK93 software package [6]. The method applied was a filtered back-projection. The cosine filter had a cut-off frequency of 0.5 and Lagrange interpolation was used to fill in missing points.

After, 573×531 neutron radiography images were produced and all the 531 cross-sections were reconstructed. In Fig. 6, the b cross-section shows the position of the ventil screw. The c cross-section shows the ventil screw and filling screws. In addition, the fastening Seger ring is easily seen here. In the d cross-section, an irregular oil distribution can be seen between the neighbouring pairs of metal plates. Nearby, the e cross-section shows two little air bubbles between the metal elements. For the f and g cross-sections, other

residual oil patterns are noticeable between the metal plates.

In the gamma-ray projection case, the images produced had dimensions of 467×427 and the number of reconstructed cross-sections was 427. The exposure time was 1 s/projection image. A sample projection image of the sequence after preprocessing is shown in Fig. 7a.

In this case, no information was obtained about the distribution of the silicon oil because the attenuation coefficient for the gamma radiation was very low. However, many details of the metal part of the VISCO clutch are observable in the b–g cross-sections of Fig. 7. In the b cross-section, we can see the ventil screw of the clutch, while in the c cross-section the ventil screw, filling screws and the fastening Seger ring are readily discernible. The metal plate (which is driven by the crank shaft) is visible in the d cross-section. A 1-mm gap appears between the neighbouring pairs of metal plates in

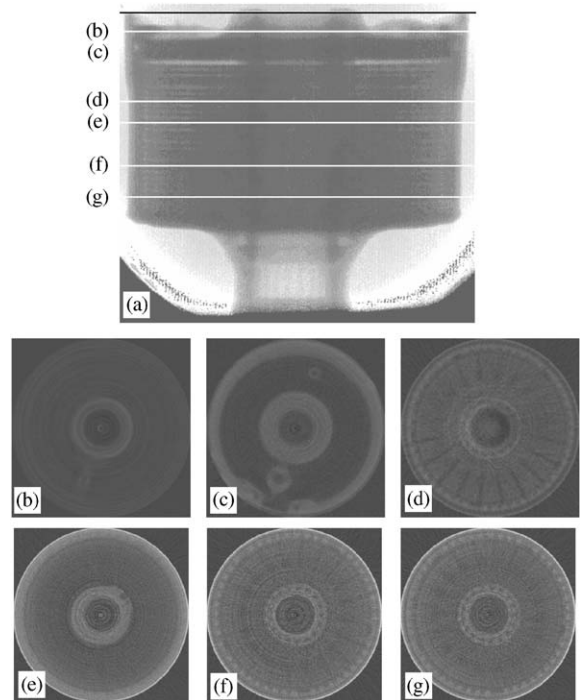


Fig. 7. Results of the reconstruction of the VISCO clutch using 180 gamma images. (a) One of the projection images after intensity and uniformity corrections and (b–g) cross-sections reconstructed by filtered back-projection using a cosine filter.

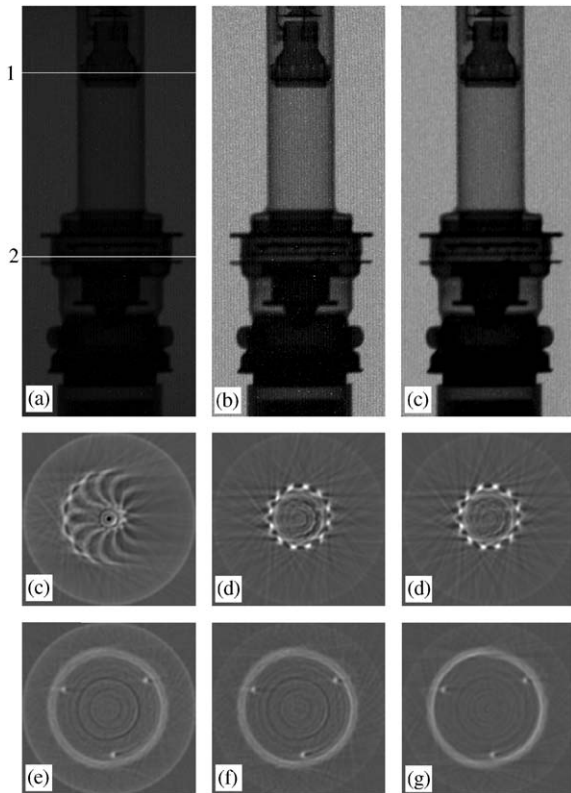


Fig. 8. The effects of the correction steps using the X-ray images of the Vidicon tube. (a) One of the original X-ray radiography images where the first cross-section shows the cooling gaps of the electron gun, while the second shows the cross-section of the accelerator rings. First column: Original projection. Second column: Images after correction step 3. Third column: Images after correction step 4. First row: Projection images. Second row: reconstructed cross-sections denoted by line 1. Third row: reconstructed cross-sections denoted by line 2.

the e cross-section. Two different metal plates of the VISCO clutch housing—which supplies torque to the wheels of a vehicle—are shown in the f and g cross-sections.

4.3. Vidicon tube

The wall of the Vidicon tube was only 0.3 mm and covered with 0.01 mm of getter material. The electrodes for the electron focusing system were both made from a tungsten alloy.

X-ray tomography was used to probe the inner structure of the Vidicon tubes, as shown in Fig. 8. Two cross-sections of the Vidicon tube are shown after applying the appropriate image correction steps. The X-ray power output was $120 \text{ kV} \times 2.5 \text{ mA}$, the exposure time was 10 s and the collimator ratio (L/D) was 200.

5. Summary

A new 3D CT facility was designed and built at the Budapest research reactor site. A unique aspect of this device is that it can make use of two types of radiation from the reactor core as well as X-ray radiation produced by a portable generator. The silicon oil distribution in the Visco clutch could be seen in the neutron radiography pictures. The metal components could also be seen in the gamma-ray images of the clutch. As for the high-resolution X-ray pictures, these revealed the details of the electrode system in the Vidicon tube. The reconstruction of the objects under investigation was carried out using the classical filtered back-projection method and DT optimization algorithms. Our novel procedure and the experimental set-up satisfy the requirements of research work and can definitely be applied in the testing of industrial products.

Acknowledgments

This work was supported by the NSF Grant DMS 0306215 (Aspects of Discrete Tomography).

References

- [1] G.T. Herman, A. Kuba (Eds.), *Discrete Tomography, Foundations, Algorithms, and Applications*, Birkhäuser, Boston, 1999.
- [2] M. Balaskó, E. Sváb, L. Cser, *NDT Int.* 20 (1987) 157.
- [3] Balaskó, E. Sváb, *Nucl. Instr. and Meth. A* 377 (1996) 140.
- [4] M. Balaskó, E. Sváb, G. Endröczi, L. Komlódi, I. Szikra, *Nondestr. Test. Eval.* 16 (2001) 297.
- [5] A. Kuba, L. Rodek, Z. Kiss, L. Ruskó, A. Nagy, M. Balaskó, *Proc. ITMNR* (2004) 140.
- [6] Homepage of SNARK93: <http://www.cs.gc.cuny.edu/~gherman/snark2001.html>.